Preprint; view final version and cite as *J. Phys. Chem. Lett.* **7** (2016) 4530-4534

The energy of liposome patch adhesion to the pipette glass determined by confocal fluorescence microscopy

Yoshitaka Nakayama[1], Radomir I. Slavchov[2,3], Navid Bavi[1,4], Boris Martinac[1,4]

[1]Mechanosensory Biophysics Laboratory, Victor Chang Cardiac Research Institute, Darlinghurst, New South Wales 2010, Australia;

[2]Department of Physical Chemistry, Sofia University, 1 J. Bourchier Blvd., Sofia 1126, Bulgaria;

[3]Department of Chemical Engineering and Biotechnology, Cambridge University, Pembroke Street, New Museums Site, CB2 3RA Cambridge, United Kingdom

[4]St. Vincent's Clinical School, University of New South Wales, Darlinghurst, New South Wales 2052, Australia;

ABSTRACT (129/150 words)

The formation of gigaseal in the patch-clamp technique is dependent on the adhesion between cell membrane and glass pipette. After gigaseal formation, the patch membrane creeps upward the pipette by the capillary force acting on a liposome bilayer. In this study, we describe a method for measuring the adhesion free energy σ_{adh} of the azolectin liposome bilayer to the pipette glass based on compensation of the capillary force acting via external pressure pushing the patch membrane backwards by using fluorescent microscopy. We measure the immobilization point at various salt concentrations and pH and determine 0.55 ± 0.07 mJ/m^2 of σ_{adh} at the condition of 320 mM ionic strength, pH 7.2. This static method provides more precise measurement for adhesion energy σ_{adh} acting on a liposome bilayer than dynamic methods.

TOC GRAPHICS

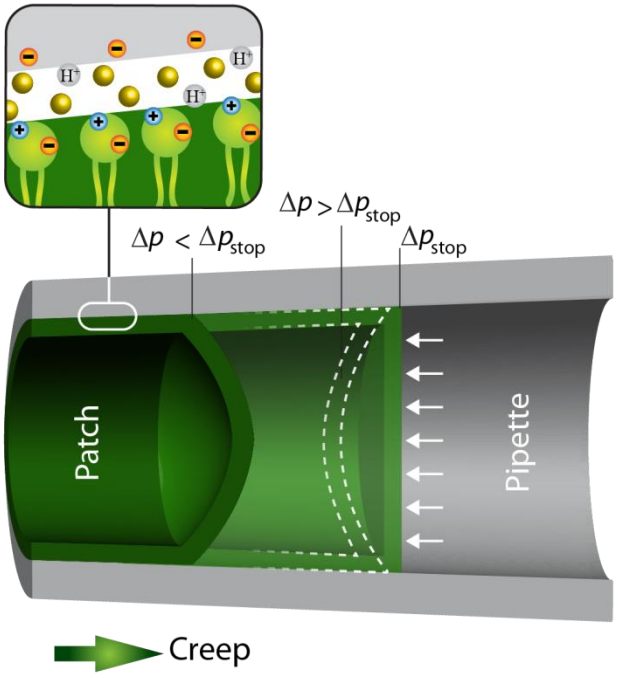

KEYWORDS (6/6 keywords**)**

gigaseal, adhesion energy, azolectin, liposome, confocal microscopy, fluorescence

Cell adhesion is an important process cells use to interact with each other and attach to a substrate [1,2]. For many years, biophysicist have studied it as well as tried to manipulate it [3,4]. Cells and bacteria adhere to surfaces using a variety of mechanisms, which are subject of intensive research [1,2]. Many basic experimental procedures involving biomembranes require tight control of adhesion. For instance, the adhesion of cells onto solid surfaces is widely used as a method for extraction of plasma membrane [5,6]. The patch-clamp is another technique, which depends on the existence of adhesion forces promoting the tight contact between the membrane and the patch pipette ensuring the formation of the gigaseal between the bilayer and the glass [7,8]. A number of studies by patch-clamp electrophysiologists focused on estimation of the lipid-glass adhesion energy and on the analysis of its conjugation with the membrane tension that activates mechanosensitive channels in a patch membrane [7,9,10].

The basic characteristic of the adhesion of a cell or a liposome to the glass is their adhesion energy σ_{adh}. It is defined as the difference between the free surface energy of the free membrane and glass surfaces ($\sigma^{\text{M}} + \sigma^{\text{G}}$) and the free energy of the membrane adhered to the glass ($\sigma^{\text{M}} + \sigma^{\text{G}} - \sigma_{\text{adh}}$). Several methods for measurement of the adhesion energy have been proposed. The classical one [11] is based on Young's balance at the 3 phase contact (3PC; Fig. 3 in S2):

$$\sigma_{\text{adh}} / \sigma^{\text{M}} = 1 + \cos\theta_{\text{eq}} \qquad (1)$$

Here θ_{eq} is the equilibrium contact angle of the adhered cell or liposome. Contact angle measurements can therefore be used for the determination of σ_{adh}, provided that the membrane tension σ^{M} is known. However, careful measures must be taken to eliminate 3PC line creep since the dynamic contact angle (advancing or receding) vary greatly with creep velocity [12]. The shape of a liposome adhered onto a solid must relax to the equilibrium contact angle in order Eq (1) to be applicable. In a capillary, the establishment of this equilibrium is complicated. A meniscus climbing into a vertical capillary has a dynamic contact angle different from θ_{eq} until Jurin's equilibrium capillary uphold height is reached [13]. In a horizontal capillary, the meniscus moves with non-zero velocity until the whole capillary is filled – the contact angle is function of this velocity and θ_{eq} may never be actually observed.

Several other methods for determination of σ_{adh} exist. Smith et al. proposed a method based on the balance between tether formation and adhesion [14]. In another study [15], the velocity $v_L \equiv$

dL/dt of creep of patches in a patch-clamp pipette was related to the driving force (adhesion and/or applied pressure) of the creep:

$$v_L = \left(\sigma_{\mathrm{adh}} - R_{\mathrm{c}}\Delta p/2\right)/k_\eta . \qquad (2)$$

Here L is the length of the glass pipette that has bilayer adhered (Fig. 1); R_{c} is the radius of the pipette at the 3PC; Δp is the applied pressure (suction pressure in the capillary corresponds to negative sign of Δp), and k_η is a friction coefficient related to the mechanism of creep and the geometry of the pipette [15]. Eq (2) was used to determine σ_{adh} together with k_η for azolectin liposomes in contact with glass [15]. This was done by measuring first v_L at $-\Delta p >> 2\sigma_{\mathrm{adh}}/R_{\mathrm{c}}$ (which allows the determination of k_η) and then v_L at $\Delta p = 0$ (once k_η is known, this yields σ_{adh}). This method yielded reasonable values for σ_{adh}, but has nevertheless disadvantages – most importantly, various kinetic effects such as non-linear force-velocity dependence [12,13] and dome bulging may result in a dependence of k_η on v_L, ultimately leading to inaccurate results.

In addition, there are several widely used methods that measure quantities directly related to the adhesion energy. For example, Priel et al. [16] utilized AFM to measure glass-membrane interactions, which are proportional to σ_{adh}. The traditional measure of cell adhesion – the number of adhered cells [3,5] – is proportional to the Boltzmann factor $\exp(-a\sigma_{\mathrm{adh}}/k_{\mathrm{B}}T)$, where a is the cell-solid contact area. In another method, an *apparent* adhesion energy $\sigma_{\mathrm{adh,n}}$ is determined as a force normal to the glass surface, balancing the normal component $\sigma^{\mathrm{M}}\sin\theta$ of the membrane tension in Fig. 3 in S2. From the assumed balance $\sigma^{\mathrm{M}}\sin\theta = \sigma_{\mathrm{adh,n}}$, a value of $\sigma_{\mathrm{adh,n}}$ follows [17,7]. This treatment neglects the elastic answer of the solid substrate [18] which is normally stiffer. In addition, the relation between $\sigma_{\mathrm{adh,n}}$ and σ_{adh} is not straightforward ($\sigma_{\mathrm{adh,n}} = \lambda/R_{\mathrm{c}}$ where λ is the line tension, which is the linear Gibbs excess of the adhesion energy σ_{adh} [19]).

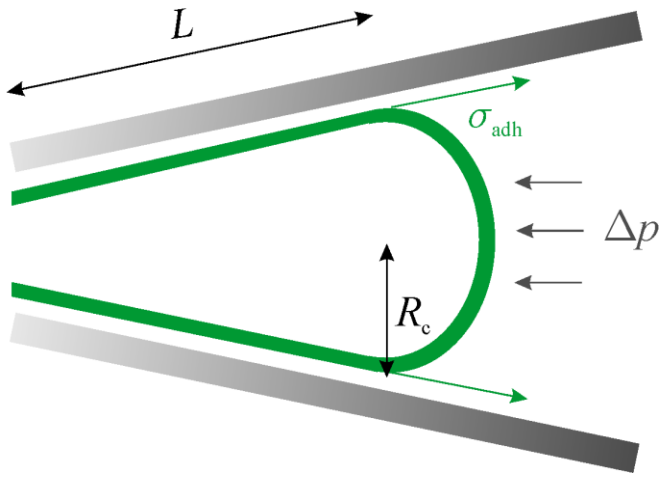

Fig. 1. Geometry of a liposome in a conical capillary.

The dynamic complications with the force balance at the 3PC line result in significant variations in the experimental results for σ_{adh} in the literature. For example, Ursell et al. [10] reported that the adhesion energy they determined for lipid bilayers on glass could vary by a factor of 2-3 for the same lipid mixture and glass. The difference between their σ_{adh} and the values from the dynamic method in Ref. [15] is nearly one order of magnitude, although the studied bilayers are similar. Therefore, a robust method is needed that does not have these issues.

It was observed in Ref [15] that from Eq (2) it follows that the patch can be immobilized by compensating the adhesion force by applying counteracting positive pressure Δp after the gigaseal is formed between the patch and the pipette – according to Eq (2), the creep velocity is zero when

$$\Delta p = 2\sigma_{adh} / R_c \qquad \left(\equiv \Delta p_{stop}\right). \tag{3}$$

This equation can be obtained easily by balancing the force acting on the dome rim ($2\pi R_c \sigma_{adh}$) with the external force applied to the patch ($\pi R_c^2 \Delta p$). Eq (3) can be utilized in a static technique for measuring σ_{adh}, in which the pressure in the patch-clamp capillary Δp is varied until $v_L = 0$ (*mechanical compensation of the capillary force*), with obvious advantages over the dynamic method of Ref [15].

In this study, we demonstrate the possibilities of this new method by measuring the adhesion energy of a bilayer to glass for relatively simple systems. We applied the technique to measure σ_{adh} of azolectin liposomes to borosilicate glass pipettes (Fig. 1 gives the approximate geometry).

Two series of experiments were performed: one in which the ionic strength of the saline solutions has been varied at fixed pH, and another with varying pH.

The measurements showed that the adhesion energy depends only weakly on the electrolyte concentration, cf. Fig. 2B and Table 1 in S3: the increase of KCl from C_{KCl} = 100 to 500 mM (with 5 mM HEPES-KOH buffer and 40 $MgCl_2$ in addition, used as usually [20] to facilitate the gigaseal formation) results into a rather small increase of σ_{adh} from 0.5 to 0.7 mJ/m^2 (i.e. 0.5 to 0.7 mN/m) (at precision ±0.1 mJ/m^2). This finding agrees with the results of Priel *et al.* for the adhesion force acting between membrane and glass [16] – these authors observed unexpectedly little effect from NaCl in the concentration range 0.1-1000 mM. The weak dependence on electrolyte concentration can be qualitatively explained within the framework of the DLVO theory, under the hypothesis that the seal (the aqueous film between the glass and the membrane) is very thin, having thickness h smaller than the Debye length L_{D} of the solution. The formulae for the electrostatic repulsion in an asymmetric film (aqueous solution of 1:1 electrolyte) of thickness $h < L_{\mathrm{D}}$ with surfaces of constant surface charge density are summarized in Ref [15] (*eqs A18-A20*). In S4, we derive the respective series for the electrostatic contribution σ_{el} to the adhesion energy at $h \to 0$, under the assumption for relatively high surface potentials ϕ:

$$\sigma_{\mathrm{el}} \approx -2k_{\mathrm{B}}T\left(\Gamma^{\mathrm{M}} + \Gamma^{\mathrm{G}}\right) + \mathrm{O}(\phi^0) + \mathrm{O}(h^1)\,. \qquad (4)$$

The leading term in this expansion is *concentration-independent*, as the adsorbed charge densities Γ^{M} at the membrane and Γ^{G} at the glass do not change significantly with C_{KCl} (which is physically equivalent to Γ^{M} & Γ^{G} being independent of h). The increase of C_{KCl} leads to an increase of σ_{adh} through second-order effects only. Yet, even these second-order effects are large enough to result in a decrease (in absolute value) of the repulsive σ_{el} by about 0.5 mJ/m^2 (equivalent to tension exerted on the membrane of 0.5 mN/m) at the highest concentration compared to the lowest, cf. Table 3 in S4. The observed increase of the total energy σ_{adh} with C_{KCl} is only 0.1-0.2 mJ/m^2 instead. A probable reason for the difference between the two is that the electrolyte also screens [21] the attractive dispersion glass-membrane interaction, leading to decrease of the respective positive contribution σ_{vdW} to σ_{adh}. If the addition of 400 mM KCl decreases the van der Waals attraction by ~20% (proportionally to the numbers in Ref. [21]), and if σ_{adh} is of the order of 0.2-0.5×σ_{vdW} [15], then the decrease of σ_{adh} due to this effect would be ~0.2-0.6 mJ/m^2, compensating

a significant part of the respective decrease of $|\sigma_{el}|$. Another factor is that the electrolyte weakens the Mg^{2+} bridges binding glass and membrane [22,23], but the magnitude of this effect cannot be estimated easily.

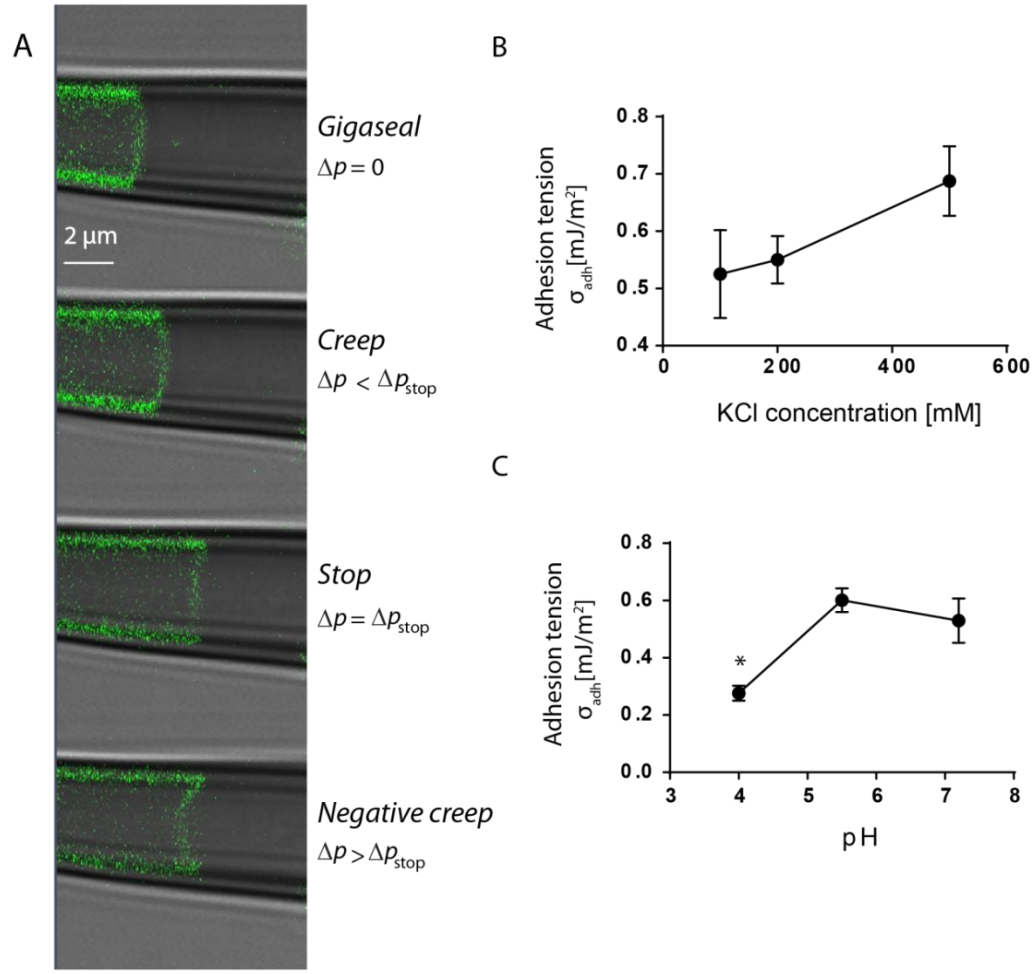

Fig. 2. (A) Patch creep inside the pipette. Positive pressure is applied to the outer wall of the patch to counteract the adhesion-driven membrane creep. (B) Effect of the concentration of KCl on the adhesion energy σ_{adh} of azolectin bilayer to the glass (40 mM $MgCl_2$, 5 mM HEPES-KOH, pH = 7.2). (C) Effect of the pH on σ_{adh} (100 mM KCl, 40 mM $MgCl_2$, 5 mM HEPES-KOH, pH adjusted by HCl). The values are Mean ± SEM. One-way ANOVA was used for statistical analysis with *p-value <0.05 and it was confirmed in groups with low n number using non-parametric Kruskal-Wallis test.

In the second series of experiments, the pH was varied at fixed ionic strength – the results for σ_{adh} are shown in Fig. 2C. We observed a maximum of the adhesion in weakly acidic solution. The observed dependence compares qualitatively well with the trend of the percentage of LM cells attached to Cytodex [11], which also reaches a maximum as a function of pH. On the other hand, the membrane-glass force measured by Priel *et al.* [16] was monotonically decreasing with pH increasing from 4 to 10.

A maximum of σ_{adh} as a function of pH may occur between the two points of zero charge, pH^{G}_{pzc} and pH^{M}_{pzc}, of the glass and the membrane (as explained qualitatively in S5). Note that in a very thin asymmetric film the points of zero charge of the two surfaces can be expected to be shifted by 1-2 units compared to the free glass and membrane surface. The reason is that the membrane surface at pH^{M}_{pzc} has zero charge, but due to the proximity of the negatively charged glass, its potential ϕ^{M} is negative instead of zero, and is of the order of the potential of the free glass surface [15]. The magnitude of this effect is estimated in S5.

The values of σ_{adh} obtained here are of the same order of magnitude as the one obtained with the dynamic method described in Ref. [15] and agree with the theoretical estimate given there. The previous value (~0.2 mJ/m^2 for azolectin membrane containing some protein) is about 3 times lower than σ_{adh} measured here at the same ionic strength in the absence of the protein. Most likely, the difference is due to the dynamic complications in Ref. [15], in particular because of the neglected dependence of k_η on v_L.

In conclusion, the adhesion energy of a lipid bilayer to the patch-clamp pipette can be measured with good precision using fluorescent microscopy for determination of the immobilization point upon mechanical compensation of the capillary force acting on a patch. The method is relatively fast, reproducible and yields results that compare well with previous experimental and theoretical estimates. The main limitation of the precision with which this method can be used is the precision with which Δp can be controlled; however, this can be significantly improved. To our knowledge, our study describes for the first time truly static method for measurement of the adhesion free energy between the lipid bilayer and the glass of the patch pipette.

Materials & methods

Liposomes consisting of azolectin (99.9%) and rhodamine-PE (0.1%) were prepared by the D/R method [24]. 2 mg of the mixture of azolectin and rhodamine-PE were dissolved in chloroform, and dried under a stream of nitrogen to make lipid films. 1 mL of D/R buffer (100-500 mM KCl, 5 mM HEPES-KOH, 40 mM $MgCl_2$, and HCl) was added. The $MgCl_2$ is needed since Mg^{2+} salt-bridges between the glass and the membrane promote formation of and stabilize the gigaseal. In the absence of HCl, pH was 7.2; we used HCl to adjust pH to 4.0 or 5.5 as determined by a pH meter (SevenEasy; METTLER TOLEDO). The lipid film was sonicated to form a liposome suspension that was transferred into a 15-mL falcon tube where further 2 mL of D/R buffer were added. After an incubation period of 2-3 hours, the solution was centrifuged at 250,000×*g*. The pellet was collected and resuspended in 60 μL of D/R buffer, then spotted onto a microscope slide and dehydrated under vacuum overnight at 25°C. The dried lipid films were rehydrated with D/R buffer for 3 h at 4°C. An aliquot of liposomes (5 μL) was placed on the bottom of the recording chamber. Unilamellar blisters emerged from the collapsed liposomes after 30 min [24,25]. Borosilicate glass pipettes (Drummond Scientific) were pulled using a Flaming/Brown pipette puller (P-87; Sutter Instruments). Glass pipette of bubble number 4.0-5.0 were used for the patch fluorescence microscopy. Fluorescence images from an inside-out excised patch membrane (similar to those in Ref [23]) were observed with a Zeiss LSM 700 confocal microscope using a long working distance water immersion objective (63×; NA 1.15; Carl Zeiss). A 555-nm laser line was used to excite the Rhodamine labeled patches with emission detected using a long pass 560-nm filter. To visualize liposome patches the pipette tip was bent to ~30° with a microforge (Narishige; MF-900) to become parallel with the bottom face of the chamber. The same saline solution was used for both pipette and bath solution. The pressure Δp applied to patch pipettes was controlled by a High Speed Pressure Clamp-1 apparatus (HSPC-1; ALA Scientific Instruments) and was monitored using a piezoelectric pressure transducer (Omega Engineering). In the absence of applied pressure, the patch was creeping up the pipette. Progressively increasing positive pressure was applied to the patch pipette until the capillary force was compensated at Δp_{stop}, Eq (3), and the liposome patch creeping stopped (no significant shift was observed for 2-3 min, and the patch dome was flat, Fig. 2A). The pressure was further increased above Δp_{stop} to confirm that the immobilization point was reached (at $\Delta p > \Delta p_{stop}$, the dome bended inward and backward creep

was observed). Each measurement was repeated with 2-3 different liposomes and different capillaries, cf. S3. With HSPC-1, the pressure can be controlled with precision of ±133 Pa (i.e. 1 mmHg). The precision of Δp presents the main limitation for the precise determination of σ_{adh}: according to eq (3), the precision of the measured σ_{adh} is $\pm 133 \times R_c/2 \sim \pm$ 0.1-0.2 mJ/m^2 (this is the main reason for the standard deviations of σ_{adh} in Table 1&Table 2 in S3).

Acknowledgements

We would like to thank Dr Frederick Sachs for his critical comments and suggestions. R.S. is grateful for funding by National Science Fund through Contract 51 from 12.04.2016 with Sofia University, N.B. has been supported by an International Scholarship from the University of New South Wales (UIPA) and B.M. is recipient of a Principal Research Fellowship from the National Health and Medical Research Council of Australia.

References

1. Zhu C.; Bao G.; Wang N. Cell mechanics: mechanical response, cell adhesion, and molecular deformation. Annu. Rev. Biomed. Eng. 2000, 2, 189-226.
2. Hori K. Adhesion of Bacteria. In: Biofilm and material science. 2015 Ch. 4.
3. Curtis A.S.G.; Forrester J.V.; McInnes C.; Lawrie F. Adhesion of cells to polystyrene surfaces. J Cell Biol. 1983 97, 1500-1506.
4. Owens N.F.; Gingell D.; Rutter P.R. Inhibition of cell adhesion by a synthetic polymer adsorbed to glass shown under defined hydrodynamic stress. J. Cell Science 1987 87, 667-675.
5. Gotlib L.J. Isolation of cell plasma membranes on microcarrier culture beads. Biochim. Biophys. Acta 1982 685, 21-26.
6. Jacobson B.S. Improved method for isolation of plasma membrane on cationic beads. Biochim. Biophys. Acta 1980 600, 769-780.
7. Suchyna, T.M.; Markin, V.S.; Sachs, F. Biophysics and structure of the patch and the gigaseal. Biophys. J. 2009, 97, 738-747.
8. Suchyna TM; Sachs F. Mechanosensitive channel properties and membrane mechanics in mouse dystrophic myotubes. J. Physiol 2007 581, 369–387.
9. Nomura T.; Cox CD.; Bavi N.; Sokabe M.; Martinac B. Unidirectional incorporation of a bacterial mechanosensitive channel into liposomal membranes. FASEB J. 2015 29, 4334-4345
10. Ursell, T.; Agrawal, A.; Phillips, R. Lipid bilayer mechanics in a pipette with glass-bilayer adhesion. *Biophys. J.* 2011 *101*, 1913-1920.
11. Absolom DR.; Lamberti FV.; Policova Z.; Zingg W.; van Oss CV.; Neumann AW. Surface thermodynamics of bacterial adhesion. Appl. Env. Microbiol. 1983 46, 90-97
12. T.D. Blake, in: C. John, Bos (Eds.), Wettability, Surfactant Science Series, vol. 49, 1993, p. 291-309.
13. Martic G.; De Coninck J.; Blake T.D. Influence of the dynamic contact angle on the characterization of porous media. J. Colloid Interface Sci., 2003 263, 213-216.
14. Smith, A.S.; Sackmann, E.; Seifert, U. Pulling tethers from adhered vesicles. *Phys. Rev. Lett.* 2004, *92*, 208101.
15. Slavchov RI.; Nomura T.; Martinac B.; Sokabe M.; Sachs F.,Gegaseal Mechanics: Creep of the gigaseal under the action of pressure, adhesion and voltage, J. Phys. Chem. B. 2014 118, 12660–12672.
16. Priel A.; Gil Z.; Moy V.T.; Magleby K.L.; Silberberg S.D. Ionic requirements for membrane-glass adhesion and giga seal formation in patch-clamp recording. Biophys. J. 2007 92, 3893-3900.
17. Opsahl L.R.; Webb W.W. Lipid-glass adhesion in giga-sealed patch-clamped membranes; Biophys. J. *19*94 *66*, 75-79.

18. Jerison ER.; Xu Y.; Wilen LA.; Dufresne ER. Deformation of an elastic substrate by a three-phase contact line. Phys Rev Lett. 2011 106, 186103.
19. Churaev NV.; Starov VM.; Derjaguin BV. The shape of the transition zone between a thin film and bulk liquid and the line tension. J. Colloid Interface Sci. 1982 89, 16-24
20. Nomura T.; Cranfield CG.; Deplazes E.; Owen DM.; Macmillan A.; Battle AR.; Constantine M.; Sokabe M.; Martinac B. Differential effects of lipids and lyso-lipids on the mechanosensitivity of the mechanosensitive channels MscL and MscS. PNAS. 2012 109, 8770–8775.
21. Petrache H.I.; Zemb T.; Belloni L.; Parsegian V.A. Salt screening and specific ion adsorption determine neutral-lipid membrane interactions. PNAS 2006 103, 7982–7987.
22. Cremer P.S.; Boxer S.G. Formation and Spreading of Lipid Bilayers on Planar Glass Supports. *J. Phys. Chem. B* 1999 103, 2554-2559.
23. Bavi N.; Nakayama Y.; Bavi O.; Cox CD.; Qin QH.; Martinac B. Biophysical implications of lipid bilayer rheometry for mechanosensitive channels. *PNAS* 2014 111, 13864–13869.
24. Häse CC.; Le Dain AC.; Martinac B. Purification and functional reconstitution of the recombinant large mechanosensitive ion channel (MscL) of *Escherichia coli*. J. Biol. Chem. 1995 270, 18329-18334.
25. DelcourA.H.; Martinac B.; Adler J.; Kung C. Modified reconstitution method used in patch-clamp studies of *Escherichia coli* ion channels. Biophys. J. 1989 56, 631–636.

Supplementary information

S1. List of symbols and abbreviations

3PC	three phase contact
C	ionic strength, $\Sigma Z_i^2 C_i/2$
C_i	concentration of the i^{th} ion
C_{KCl}	concentration of KCl
e	elementary charge
h	thickness of the seal
k_{B}	Boltzmann constant
k_η	friction coefficient
L	wetted length of the capillary, Fig. 1
L_{D}	Debye length, $L_{\text{D}} = (k_{\text{B}}T\varepsilon/2e^2C)^{½}$
pH_{pzc}	point of zero charge
Δp	applied pressure in the patch pipette
Δp_{stop}	the pressure at which creep stops, Eq (3)
R_{c}	radius of the capillary at the 3PC, Fig. 1
T	temperature [K]
t	time
v_L	creep velocity, $v_L = \text{d}L/\text{d}t$
Z_i	valence of the i^{th} ion
Γ^{G}, Γ^{M}	adsorbed charge density at the glass and the outer bilayer surface
ε	absolute dielectric permittivity
θ	three phase contact angle
θ_{eq}	Young's equilibrium three phase contact angle
σ_{adh}	the adhesion energy ($\sigma_{\text{adh}} > 0$)
σ_{el}	electrostatic contribution to the adhesion energy
σ_{el0}	electrostatic contribution to the adhesion energy for surfaces in contact
σ^{G}	the surface tension of the glass
σ^{M}	membrane tension

σ_{vdW} dispersion contribution to the adhesion energy

Φ^M, Φ^G $= \exp(-e\phi^M/k_BT)$, $\exp(-e\phi^G/k_BT)$

Φ_m $= \exp(-e\phi_m/k_BT)$

ϕ^M, ϕ^G surface potentials of the outer wall of the bilayer and the glass surface

ϕ^M_∞, ϕ^G_∞ surface potentials of the outer wall of the free bilayer and the free glass surface

ϕ_m the minimal potential in the film

subscripts:

adh adhered membrane

c capillary

superscripts:

G glass

M membrane

S2. Young's equation for the adhered patch

In this supplement we are clarifying the definition of three phase contact angle, cf. Fig. 3, and we derive the relation between adhesion energy and θ [11]. Young's balance in direction tangential to the glass surface in Fig. 3 reads:

$$\sigma^{\mathrm{G}} = \sigma^{\mathrm{G}} + \sigma^{\mathrm{M}} - \sigma_{\mathrm{adh}} + \sigma^{\mathrm{M}} \cos\theta_{\mathrm{eq}} \,. \tag{5}$$

This equation is equivalent to Eq. (1).

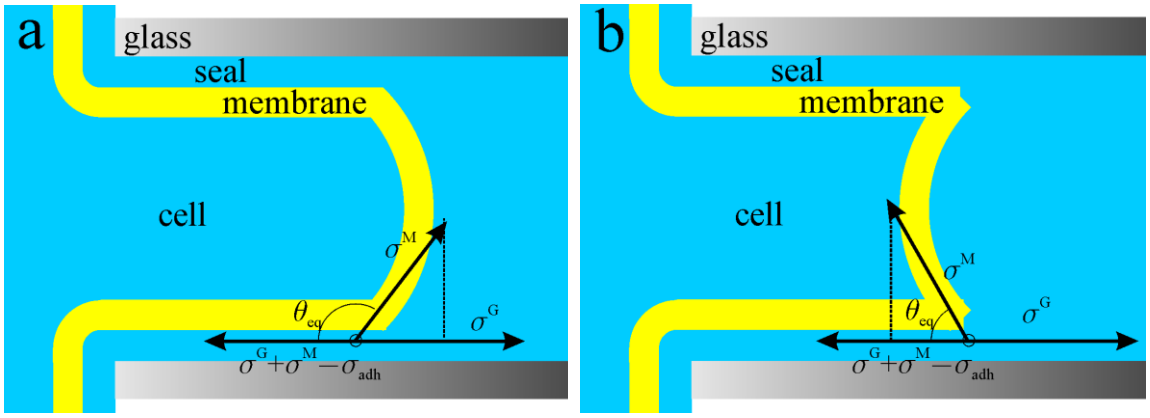

Fig. 3. Young's balance at the 3 phase contact region (3PC). If $\sigma_{\mathrm{adh}} < \sigma^{\mathrm{M}}$, then from Eq (1) it follows that $\theta_{\mathrm{eq}} > 90^{\mathrm{o}}$ as in figure a. For $\sigma_{\mathrm{adh}} > \sigma^{\mathrm{M}}$, the equilibrium 3PC angle will be $\theta_{\mathrm{eq}} < 90^{\mathrm{o}}$ as in figure b.

S3. Experimental data

In this supplement, we summarize the data obtained for the adhesion free energy by the patch immobilization fluorescence microscopy method – Table 1 for $\sigma_{adh}(C_{KCl})$ and Table 2 for σ_{adh}(pH). The averaged values and the standard errors of the mean are given in Fig. 2B&C.

Table 1. Adhesion energy of azolectin liposomes (with 0.1% rhodamine-PE) to glass at various electrolyte concentrations. All solutions contained also 40 mM $MgCl_2$, and 5 mM HEPES-KOH; pH = 7.2.

KCl [mM]	**Δp [Pa]**	**R_c [μm]**	**σ_{adh} [mJ/m^2]**
100	667	1.50	0.50
100	533	1.25	0.33
100	667	2.10	0.70
100	533	2.20	0.59
ionic strength* C = 220 mM		Average σ_{adh} ± st. dev.: 0.53±0.15	
200	400	2.50	0.50
200	533	2.00	0.53
200	800	1.60	0.64
ionic strength* C = 320 mM		Average σ_{adh} ± st. dev.: 0.55±0.07	
500	800	1.76	0.70
500	933	1.83	0.85
500	800	1.50	0.60
500	667	1.78	0.59
ionic strength* C = 620 mM		Average σ_{adh} ± st. dev.: 0.69±0.12	

* HEPES contribution is neglected.

Table 2. Adhesion energy of azolectin liposome (with 0.1% rhodamine-PE) to glass at various pH. All solutions contained 100 mM KCl, 40 mM $MgCl_2$, and 5 mM HEPES-KOH; pH was adjusted with HCl.

pH	**Δp [Pa]**	**R_c [μm]**	**σ_{adh} [mJ/m^2]**
4	267	2.10	0.28
	400	1.15	0.23
	533	1.20	0.32
	Average σ_{adh} ± st. dev.: 0.28±0.05		
5.5	667	2.05	0.68
	800	1.40	0.56
	533	2.10	0.56
	Average σ_{adh} ± st. dev.: 0.60±0.07		
7.2	667	1.50	0.50
	533	1.25	0.33
	667	2.10	0.70
	533	2.20	0.59
	Average σ_{adh} ± st. dev.: 0.52±0.15		

S4. Electrostatic repulsion in very thin films

In this supplement, we estimate the effect of the electrolyte concentration on the electrostatic contribution σ_{el} to the adhesion energy. We consider a simplified model: the seal is assumed to be an asymmetric film of homogeneously charged surfaces. Its thickness h is smaller than the Debye length L_D of the solution. The role of the inner wall of the membrane is neglected [15]. For simplicity, we neglect also the role of the 40 mM divalent ions – we assume that the repulsion in a seal containing 40 mM $MgCl_2$ and 100-500 mM KCl is approximately the same as with seal containing only KCl of the same ionic strength (C = 220-620 mM). The contribution of HEPES-KOH and HCl to the ionic strength is small and is neglected as well. The formulae for the electrostatic repulsion in an asymmetric film (aqueous solution of 1:1 electrolyte) of thickness $h < L_D$ with surfaces of constant surface charge density are summarized in Ref [15] (*eqs A18-A20*). Here we derive the respective formulae for the adhesion energy.

For the relation between the thickness of the film and the minimal potential ϕ_m in the film we previously derived [15]:

$$\frac{h}{L_D} = \frac{h^{Mm}}{L_D} + \frac{h^{Gm}}{L_D} \approx 2\frac{\sqrt{\Phi^M - \Phi_m}}{\Phi_m} + 2\frac{\sqrt{\Phi^G - \Phi_m}}{\Phi_m}. \qquad (6)$$

Here, $\Phi_m = \exp(-e\phi_m/k_BT)$, ϕ_m is the minimal potential (in a symmetric film, it lays in the middle of the film – Langmuir's "midplane potential" – but with asymmetric films such as the water film between glass and membrane this is not the case); $\Phi^M \equiv \exp(-e\phi^M/k_BT)$ and $\Phi^G \equiv \exp(-e\phi^G/k_BT)$; $L_D = (k_BT\varepsilon/2e^2C)^{1/2}$ is the Debye length, e is elementary charge, ε is the absolute dielectric permittivity; h^{Mm} and h^{Gm} are the distances from the surface of minimal potential to the membrane and the glass surface, respectively. Note that *eq A19* in Ref [15] has a typographical error – Eq (6) here is the correct one.

The electrostatic adhesion free energy follows from the integration of the tangential stress tensor in the diffuse part of the double layer [26] (in the approximation for constant surface charge, the adsorption layer contribution to the total seal tension does not change, but it will be important for the constant potential and the charge regulation regimes). The diffuse layer contribution to the seal tension is the sum of two contributions,

$$\sigma_{\mathrm{el}}^{\mathrm{Mm}} = -2k_{\mathrm{B}}TCL_{\mathrm{D}} \int_{\Phi_{\mathrm{m}}}^{\Phi^{\mathrm{M}}} \frac{1}{\Phi}\sqrt{\Phi + \frac{1}{\Phi} - \Phi_{\mathrm{m}} - \frac{1}{\Phi_{\mathrm{m}}}}\,\mathrm{d}\Phi \xrightarrow{h\to 0} -\frac{4}{3}k_{\mathrm{B}}TCL_{\mathrm{D}}\frac{\left(\Phi^{\mathrm{M}} - \Phi_{\mathrm{m}}\right)^{3/2}}{\Phi_{\mathrm{m}}}, \text{ and}$$

$$\sigma_{\mathrm{el}}^{\mathrm{Gm}} = -2k_{\mathrm{B}}TCL_{\mathrm{D}} \int_{\Phi_{\mathrm{m}}}^{\Phi^{\mathrm{G}}} \frac{1}{\Phi}\sqrt{\Phi + \frac{1}{\Phi} - \Phi_{\mathrm{m}} - \frac{1}{\Phi_{\mathrm{m}}}}\,\mathrm{d}\Phi \xrightarrow{h\to 0} -\frac{4}{3}k_{\mathrm{B}}TCL_{\mathrm{D}}\frac{\left(\Phi^{\mathrm{G}} - \Phi_{\mathrm{m}}\right)^{3/2}}{\Phi_{\mathrm{m}}}, \qquad (7)$$

which are the integrals of the Maxwell stress tensor from the surface of minimal potential to the membrane and the glass surface, respectively (compare to h^{Mm} and h^{Gm} [15]). For the calculation of the integrals, we used that for a very thin film, Φ_{m}, Φ^{M} and Φ^{G} tend to the same value [15]. For the diffuse layer at the outer wall of the *free* membrane and the *free* glass surface, we find:

$$\sigma_{\mathrm{el}\infty}^{\mathrm{M}} = -2k_{\mathrm{B}}TCL_{\mathrm{D}} \int_{1}^{\Phi_{\infty}^{\mathrm{M}}} \frac{1}{\Phi}\sqrt{\Phi + \frac{1}{\Phi} - 2}\,\mathrm{d}\Phi = -4k_{\mathrm{B}}TCL_{\mathrm{D}}\left(\sqrt{\Phi_{\infty}^{\mathrm{M}}} + \frac{1}{\sqrt{\Phi_{\infty}^{\mathrm{M}}}} - 2\right) \quad \text{and}$$

$$\sigma_{\mathrm{el}\infty}^{\mathrm{G}} = -4k_{\mathrm{B}}TCL_{\mathrm{D}}\left(\sqrt{\Phi_{\infty}^{\mathrm{M}}} + \frac{1}{\sqrt{\Phi_{\infty}^{\mathrm{M}}}} - 2\right), \qquad (8)$$

where, $\Phi_{\infty}^{\mathrm{M}} = \exp(-e\phi_{\infty}^{\mathrm{M}}/k_{\mathrm{B}}T)$, $\Phi_{\infty}^{\mathrm{G}} = \exp(-e\phi_{\infty}^{\mathrm{G}}/k_{\mathrm{B}}T)$, and $\phi_{\infty}^{\mathrm{M}}$ and $\phi_{\infty}^{\mathrm{G}}$ are the surface potentials of the free membrane and the glass surfaces (at $h \to \infty$). Eqs (8) are classical results from Gouy's model. By definition, the electrostatic contribution to σ_{adh} is:

$$\sigma_{\mathrm{el}} = \sigma_{\mathrm{el}\infty}^{\mathrm{M}} + \sigma_{\mathrm{el}\infty}^{\mathrm{G}} - \sigma_{\mathrm{el}}^{\mathrm{Mm}} - \sigma_{\mathrm{el}}^{\mathrm{Gm}}. \qquad (9)$$

For very thick film, it follows from Eqs (7)&(8) that $\sigma_{el}^{m} \to \sigma_{el\infty}$ both for the glass and the membrane, and $\sigma_{el} \to 0$. For very thin film, $\sigma_{el}^{m} \to 0$ (infinitely thin diffuse layer) and therefore,

$$\sigma_{el} \xrightarrow{h\to 0} \sigma_{el\infty}^{M} + \sigma_{el\infty}^{G} \qquad \left(\equiv \sigma_{el0}\right), \tag{10}$$

i.e., at contact, two surfaces of constant charge will have electrostatic adhesion energy equal to the free energy σ_{el0} of the two electric diffuse layers of the two free surfaces. Therefore, σ_{el} has a value between the minimal one – σ_{el0} – corresponding to infinitely thin film (note that $\sigma_{el0} < 0$) and a maximal value 0 for thick film.

The generalized Gouy equations for the two walls of the film in the considered approximation are given by *eq A18* in Ref [15]:

$$\Phi^{M} = \Phi_{m} + \left(\Phi_{\infty}^{M} + \frac{1}{\Phi_{\infty}^{M}} - 2\right); \qquad \Phi^{G} = \Phi_{m} + \left(\Phi_{\infty}^{G} + \frac{1}{\Phi_{\infty}^{G}} - 2\right). \tag{11}$$

We substitute this into Eq (6) and solve it for Φ_m; the result is:

$$\Phi_{m} = 2\left(\sqrt{\Phi_{\infty}^{M} + \frac{1}{\Phi_{\infty}^{M}} - 2} + \sqrt{\Phi_{\infty}^{G} + \frac{1}{\Phi_{\infty}^{G}} - 2}\right)\frac{L_D}{h}. \tag{12}$$

Substituting this formula in Eqs (7)-(9), we obtain an explicit expression for σ_{el}:

$$\sigma_{el} = \sigma_{el0} + k_B T C \gamma_h h\,, \tag{13}$$

where

$$\sigma_{el0} = -4k_B T C L_D\left(\sqrt{\Phi_{\infty}^{M}} + \frac{1}{\sqrt{\Phi_{\infty}^{M}}} + \sqrt{\Phi_{\infty}^{G}} + \frac{1}{\sqrt{\Phi_{\infty}^{G}}} - 4\right) \quad \text{and}$$

$$\gamma_h = \frac{2}{3}\frac{\left(\Phi_{\infty}^{M} + \frac{1}{\Phi_{\infty}^{M}} - 2\right)^{3/2} + \left(\Phi_{\infty}^{G} + \frac{1}{\Phi_{\infty}^{G}} - 2\right)^{3/2}}{\sqrt{\Phi_{\infty}^{M} + \frac{1}{\Phi_{\infty}^{M}} - 2} + \sqrt{\Phi_{\infty}^{G} + \frac{1}{\Phi_{\infty}^{G}} - 2}}. \tag{14}$$

Note that the surface potentials ϕ_∞^{M} & ϕ_∞^{G} of the free surfaces (and Φ_∞^{M} & Φ_∞^{G}, respectively) are functions of the ionic strength through Gouy's equations for the two surfaces:

$$\Phi_\infty^{\mathrm{M}} + \frac{1}{\Phi_\infty^{\mathrm{M}}} - 2 = \frac{e^2\left(\Gamma^{\mathrm{M}}\right)^2}{2\varepsilon k_{\mathrm{B}} TC} \quad \text{and} \quad \Phi_\infty^{\mathrm{G}} + \frac{1}{\Phi_\infty^{\mathrm{G}}} - 2 = \frac{e^2\left(\Gamma^{\mathrm{G}}\right)^2}{2\varepsilon k_{\mathrm{B}} TC}. \tag{15}$$

Using the parameters for Newton black film from Ref. [15] (h = 5 Å, ϕ_∞^{M} = –50 mV, ϕ_∞^{G} = –20 mV at 220 mM, corresponding to Γ^{M} = 0.39 nm^{-2} and Γ^{G} = 0.14 nm^{-2}), from Eq (13)-(15) we obtain the results in Table 3. As seen there, the decrease of σ_{el} upon addition of 400 mM KCl is relatively small (compared to the effects one observes with thick films of $h > L_{\mathrm{D}}$) – we expect it to be of the order of –0.39 + 0.94 = 0.55 mJ/m^2. However, even this value is larger than the observed increase of σ_{adh} in Fig. 2B (which is about 0.16 mJ/m^2). Probably, the electrolyte is screening not only the electrostatic repulsion, but it screens also the van der Waals attraction [21] thus compensating to a certain extent the change of σ_{el}.

Finally, the series of Eq (13) (calculated with the help of Eqs (14)&(15)) at $h \to 0$ and large Φ_∞^{M} & Φ_∞^{G} >> 1 lead to Eq (4).

Table 3. Calculated electrostatic contribution σ_{el} to the adhesion energy at pH = 7.2.

C [mM]	ϕ_∞^{M} [mV]	ϕ_∞^{G} [mV]	σ_{el} [mJ/m^2]
220	–50	–20	–0.94
320	–43	–17	–0.73
620	–33	–12	–0.39

S5. Effect of the pH and shift of the point of zero charge with thickness

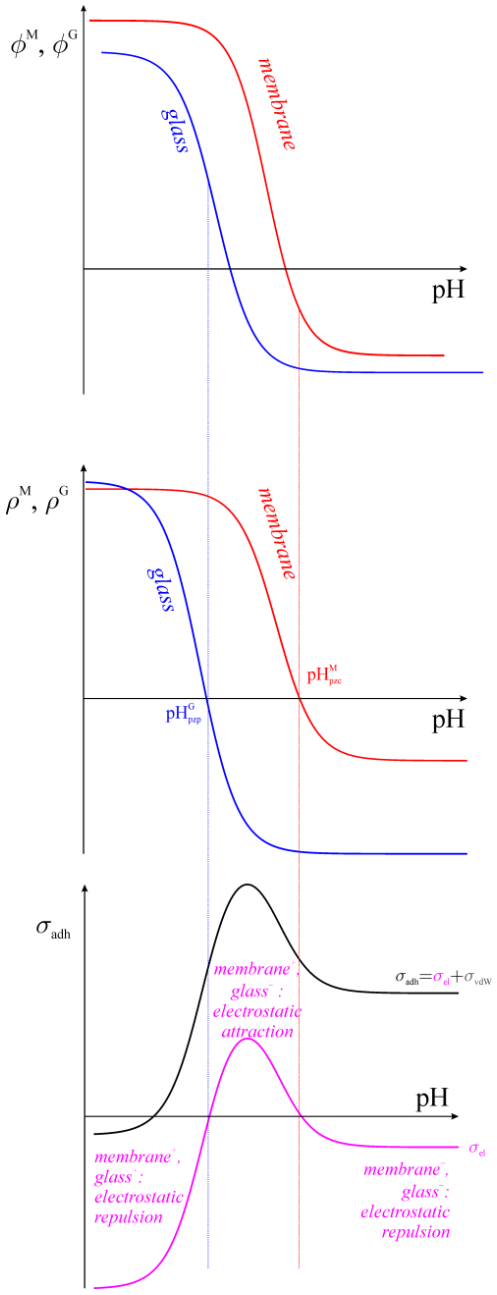

Fig. 4. Schematic dependence of the surface potentials (up), surface charge densities (middle) and σ_{el} (down) on pH. Membrane's ρ^M (pink) and glass' ρ^G (blue) change sign (positive at low pH, negative at high). The point of zero charge of the bilayer wall is expected to be at higher pH compared to the glass. The electrostatic adhesion energy σ_{el} is proportional to $-\rho^M \times \rho^G$ and changes sign at both pzc. The surface potential ϕ^M is negative at pH^M_{pzc}, due to the proximity of the

negatively charged glass. The surface potential ϕ^{G} is positive at pH^{G}_{pzc}, due to the positively charged bilayer.

Both glass and membrane are protonated at low pH (they carry positive charge ρ^{G} and ρ^{M} there). Both are expected to be negatively charged at high pH. We expect the point of zero charge to be higher for the lipid. This situation is illustrated qualitatively in Fig. 4 (*centre*). The electrostatic contribution σ_{el} to the adhesion energy is proportional [26] to $-\rho^{G}\rho^{M}$ (Fig. 4-*down*, the pink line). It is negative (repulsive) above membrane's point of zero charge and below glass' point of zero charge, and positive (attractive) in between. The total adhesion energy σ_{adh} has also the positive pH-independent contribution from vdW and other attractive interactions, which lead to $\sigma_{adh} > 0$ at the points of zero charge. The black curve for σ_{el}(pH) in Fig. 4-*down* compares qualitatively well to Gotlib's experiment on adhesion of cells – cf. *fig. 2* in Ref. [5].

The point of zero charge occurs when the adsorbed H^{+} at the membrane compensates its negative surface charge of surface density Γ^{M}. If we assume that the adsorption of H^{+} follows Davies isotherm [27], i.e., it is a linear function of the subsurface concentration $10^{-pH}\exp(-e\phi^{M}/k_{B}T)$ of H^{+}, with adsorption constant K_{H}, we can write that at the point of zero charge of the membrane it is valid that

$$K_{H}10^{-pH^{M}_{pzc}}\exp\left(-e\phi^{M}/k_{B}T\right)=\Gamma_{M}, \tag{16}$$

where $\phi^{M} \sim -50$ mV due to the poximity of the glass (i.e., for the surfaces in a very thin film of $h < L_{D}$, the point of zero charge is not a point of zero potential – Fig. 4-*up&centre*). On the other hand, $\phi^{M} = 0$ mV for the free membrane, i.e.

$$K_{a}10^{-pH^{M}_{pzc,\infty}}=\Gamma_{M}, \tag{17}$$

where $pH^{M}_{pzc,\infty}$ is the point of zero charge of the free liposome. Combining the two equations, we obtain $pH^{M}_{pzc} = pH^{M}_{pzc,\infty} - e\phi^{M}/2.3k_{B}T$. The free membrane value for phosphatidylcholine is 4.2 [28], so pH^{M}_{pzc} =5-6. Similar reasoning applies for the glass surface: in the vicinity of its point of zero charge, the membrane is positively charged, therefore, the point of zero charge pH^{G}_{pzc} in the seal must be lower than the one of the free glass. At $pH > pH^{M}_{pzc}$ and $pH < pH^{G}_{pzc}$, the electrostatic interaction in the seal is repulsive (surface charge of the same sign); at $pH = pH^{G}_{pzc}$ and $pH = pH^{M}_{pzc}$, it is zero; at $pH^{G}_{pzc} < pH < pH^{M}_{pzc}$, it is attractive and passes through a maximum.

Supplementary references

26. Derjaguin, B.V. Theory of stability of colloids and thin films. Nauka, Moscow (1986).
27. Davies, J.T. Adsorption of long-chain ions I. Proc R Soc London, Ser A 1958, 245, 417-428.
28. Zhou Y.; Raphael RM. Solution pH alters mechanical and electrical properties of phosphatidylcholine membranes: relation between interfacial electrostatics, intramembrane potential, and bending elasticity. Biophys. J. 2007, 92, 2451-2462.